

See discussions, stats, and author profiles for this publication at: <https://www.researchgate.net/publication/272522305>

# A New Selective Chromogenic and Turn-On Fluorogenic Probe for Copper (II) in Solution and Vero Cells: Recognition of Sulphide by [CuL]

ARTICLE *in* DALTON TRANSACTIONS · FEBRUARY 2015

Impact Factor: 4.2 · DOI: 10.1039/C4DT03969F

---

READS

107

## 10 AUTHORS, INCLUDING:



[Dr. Saikat Kumar Manna](#)

Haldia Government College

18 PUBLICATIONS 105 CITATIONS

[SEE PROFILE](#)



[Rajkishor Maji](#)

Indian Institute of Engineering Science and ...

13 PUBLICATIONS 44 CITATIONS

[SEE PROFILE](#)



[Tapan Kumar Mondal](#)

Jadavpur University

136 PUBLICATIONS 971 CITATIONS

[SEE PROFILE](#)



[Dilip K Maiti](#)

University of Calcutta

48 PUBLICATIONS 455 CITATIONS

[SEE PROFILE](#)



Cite this: *Dalton Trans.*, 2015, **44**, 6490

## A new selective chromogenic and turn-on fluorogenic probe for copper(II) in solution and vero cells: recognition of sulphide by [CuL]<sup>†</sup>

Ajit Kumar Mahapatra,<sup>\*a</sup> Sanchita Mondal,<sup>a</sup> Saikat Kumar Manna,<sup>a</sup> Kalipada Maiti,<sup>a</sup> Rajkishor Maji,<sup>a</sup> Md. Raihan Uddin,<sup>b</sup> Sukhendu Mandal,<sup>b</sup> Deblina Sarkar,<sup>c</sup> Tapan Kumar Mondal<sup>c</sup> and Dilip Kumar Maiti<sup>d</sup>

A new coumarin-appended thioimidazole-linked imine conjugate, *viz.* **L** has been synthesized and characterized. **L** has been found to recognize Cu<sup>2+</sup> selectively among a wide range of biologically relevant metal ions. The chemosensing behavior of **L** has been demonstrated through fluorescence, absorption, visual fluorescence color changes, ESI-MS and <sup>1</sup>H NMR titrations. The chemosensor **L** showed selectivity toward Cu<sup>2+</sup> by switch on fluorescence among the 18 metal ions studied with a detection limit of 1.53 μM. The complex formed between **L** and Cu<sup>2+</sup> is found to be 1:1 on the basis of absorption and fluorescence titrations and was confirmed by ESI-MS. DFT and TDDFT calculations were performed in order to demonstrate the structure of **L** and [CuL] and the electronic properties of chemosensor **L** and its copper complex. This highly fluorescent [CuL] complex has been used to recognize sulphide selectively among the other allied anions. Microstructural features of **L** and its Cu<sup>2+</sup> complex have been investigated by SEM imaging (scanning electron microscopy). The biological applications of **L** were evaluated in Vero cells and it was found to exhibit low cytotoxicity and good membrane permeability for the detection of Cu<sup>2+</sup>.

Received 23rd December 2014,  
Accepted 17th February 2015

DOI: 10.1039/c4dt03969f

[www.rsc.org/dalton](http://www.rsc.org/dalton)

## Introduction

Copper is an essential trace element, the third most abundant (after Fe<sup>2+</sup> and Zn<sup>2+</sup>) in humans, and is present in low levels in a variety of cells and tissues with the highest concentrations in the liver,<sup>1</sup> and in the brain.<sup>2</sup> Copper is a redox-active nutrient that is needed at unusually high bodily levels for normal brain function.<sup>3</sup> Owing to the large oxygen capacity and oxidative metabolism of brain tissue, neurons and glia alike require copper for basic respiratory and antioxidant enzymes cytochrome *c* oxidase (CcO) and Cu/Zn superoxide dismutase (SOD1), respectively. In addition, copper is a necessary cofactor for many brain-specific enzymes that control the homeostasis of neurotransmitters, neuropeptides, and dietary amines. However, it is toxic at higher concentration levels, for example, the accumulation of Cu<sup>2+</sup> in the liver and kidney may cause

gastrointestinal disease, Wilson's disease,<sup>4</sup> amyotrophic lateral sclerosis,<sup>5</sup> Menkes syndrome,<sup>6</sup> Alzheimer's disease,<sup>7</sup> hypoglycemia, dyslexia and infant liver damage.<sup>8,9</sup> Therefore, the development of molecular turn-on fluorescent probes for fast detection of Cu<sup>2+</sup> in water or physiological samples is of toxicological and environmental concern.<sup>10</sup> However, fluorescence detection of Cu<sup>2+</sup> by a turn-on response is particularly difficult due to its paramagnetic nature,<sup>11</sup> as unpaired electrons in close proximity to fluorescent dyes tend to quench emission. Therefore several on-off fluorescent probes for Cu<sup>2+</sup> have been reported.<sup>12</sup> Recently, many fluorescent chemosensors for Cu<sup>2+</sup>-selective detection were reported and have been used with some success in biological applications.<sup>13</sup> However, some of them have shortcomings for practical application such as cross-sensitivities toward other metal cations, low water solubility, a narrow pH span, slow response, a low fluorescence quantum yield in aqueous media, and cytotoxicities of ligands. To prevent fluorescence quenching by Cu<sup>2+</sup> and to achieve a practical "off-on" imaging with a strong fluorescence response upon binding the analyte, we devised a sensor system that separates the sensing and the signaling events. Two different fluorogenic ligands capable of metal chelation are employed whereby one of the ligands binds Cu<sup>2+</sup>, while the other produces a fluorescence signal to report the binding event. Although the designed chemosensor is more effective in

<sup>a</sup>Department of Chemistry, Indian Institute of Engineering Science and Technology, Shibpur, Howrah - 711103, India. E-mail: [akmahapatra@rediffmail.com](mailto:akmahapatra@rediffmail.com); Fax: +91326684564

<sup>b</sup>Department of Microbiology, Ballygunge Science College, Kolkata-700019, India

<sup>c</sup>Department of Chemistry, Jadavpur University, Kolkata-700032, India

<sup>d</sup>Department of Chemistry, University of Calcutta, Kolkata-700009, India

<sup>†</sup>Electronic supplementary information (ESI) available. CCDC 1011197. For ESI and crystallographic data in CIF or other electronic format see DOI: 10.1039/c4dt03969f

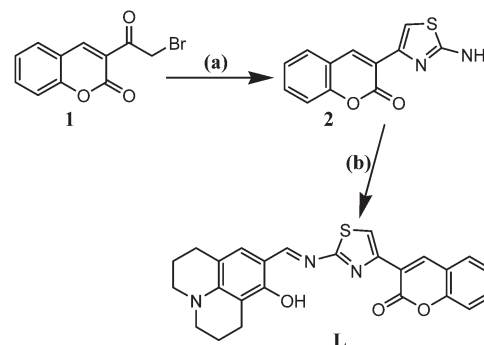
sensing  $\text{Cu}^{2+}$ , other important cations such as  $\text{Au}^{3+}$ ,  $\text{Pd}^{2+}$  and  $\text{Zn}^{2+}$  ions exhibited some fluorescence turn ON response.

Sulphide anion, as a toxic, hazardous and traditional pollutant, is widely spread in the environment. It is produced naturally and as a result of human activity. Natural sources include non-specific and anaerobic bacteria reduction of sulfates and sulfur containing amino acids in meat proteins. Sulphide anion is found naturally in crude petroleum, volcanic eruption, and hot springs. It is released from stagnant or polluted waters and manure or coal pits. Sulphide anion may be produced by a variety of commercial methods as a byproduct in industrial processes, for example, conversion into sulfur and sulfuric acid, dyes and cosmetic manufacturing, production of an agricultural disinfectant, paper and wood pulp, etc.<sup>14</sup> Therefore, it is possible to bioconcentrate and biomagnify it in the food-chain. Exposure to a high level of sulphide can lead to irritation in mucous membranes, unconsciousness, and respiratory paralysis.<sup>15</sup> Once a sulphide anion is protonated, it becomes even more toxic. Therefore, the detection of sulphide anion has become very important from an industrial, environmental, and biological point of view.<sup>16</sup> A variety of detection techniques have been developed for the determination of sulphide anion.<sup>17</sup> Among them, sulphide anion sensing by fluorescence spectrometry has received much importance due to its high sensitivity and easy detection.<sup>18</sup> However, the development of fluorescent sensors for anions in aqueous media is still a challenging task because of the strong hydration nature of anions, which weakens the interactions of the chemosensors with the target anions.<sup>19</sup> This could be avoided by using the metal displacement approach, which is based on the fact that the stability constant of a complex formed by metal-anion affinity is larger than that of the complex of a metal and its chemosensor.<sup>20</sup> Sulphide is known to react with copper ions to make a very stable  $\text{CuS}$  form with a very low solubility product constant  $K_{\text{sp}} = 6.3 \times 10^{-36}$  of the cyanide one ( $3.2 \times 10^{-20}$ ). Recently, Nagano and Zeng groups reported new approaches for the detection of sulphide in live biological systems through the development of a  $\text{Cu}^{2+}$  complex for chemoselective sulphide-responsive fluorescent sensors.<sup>21</sup> Recently, we presented a displacement-based sensing method by using metal-based ensembles for other anion recognition or sensing.<sup>22,23</sup> From this idea, we have successfully developed an ensemble of fluorescence and colorimetric sulphide chemosensors based on the traditional  $\text{Cu}^{2+}$  chemosensors.

## Results and discussion

The fluorescent chemosensor molecule (**L**) has been synthesized by two consecutive steps starting from 3-bromoacetyl-coumarin (**1**) followed by the preparation of its thiazolylamine derivative (**2**) by the condensation reaction with thiourea as shown in Scheme 1.<sup>24</sup>

The final chemosensor molecule **L** has been synthesized by the condensation of **2** with 8-hydroxy-2,3,6,7-tetrahydro-1*H*,5*H*-benzo[*ij*]quinolizine-9-carboxaldehyde (**b**) in an ethanolic



**Scheme 1** Synthesis of **L**. Reagents and conditions: (a) thiourea, dry ethanol, reflux, 12 h; (b) 8-hydroxy-2,3,6,7-tetrahydro-1*H*,5*H*-benzo[*ij*]-quinolizine-9-carboxaldehyde, dry ethanol, reflux, 6 h.

medium with 72% yield (Scheme 1).<sup>25</sup> All the intermediates and the final chemosensor molecule were characterized by various analytical and spectral techniques. The structure of **L** was well characterized by  $^1\text{H}$  NMR,  $^{13}\text{C}$  NMR, and mass spectra (Fig. S3–S5, ESI†). The molecular structure of the intermediate thiazolylamine compound **2** has been established by  $^1\text{H}$  NMR, ESI-MS as well as single-crystal XRD analysis (Fig. S1, S2 and S8, ESI†). Single crystals of **2** suitable for X-ray diffraction study were obtained by slow diffusion of methanol into a solution of **2** in chloroform and the data were collected<sup>26</sup> (Table S4, ESI†).

### UV-vis and fluorescence spectral behavior of **L**

The sensitivity of **L** toward different metal ions and its preferential selectivity toward  $\text{Cu}^{2+}$  over the other ions has been studied by fluorescence and absorption titrations.

The UV-vis absorption spectra of chemosensor **L** in aqueous acetonitrile ( $\text{CH}_3\text{CN}-\text{H}_2\text{O} = 7:3$  v/v, 10 mM HEPES buffer, pH = 7.4) are dominated by two absorption bands at 278 and 358 nm, and a low energy (LE) band centered at 446 nm attributed to the iminothiazole moiety. During titration, the concentration of **L** was kept constant at 40  $\mu\text{M}$  and the mole ratio of  $\text{Cu}^{2+}$  was varied. The absorbance of 278, 358, and 446 nm bands is found to decrease upon addition of  $\text{Cu}^{2+}$  (Fig. 1a), indicating the interaction of  $\text{Cu}^{2+}$  with the iminothiazole/aromatic moiety. The low energy (LE) band at 446 nm gradually decreases, upon addition of  $\text{Cu}^{2+}$  ions, which is responsible for the change of color from light yellow to colorless. This fact can be used for a ‘naked-eye’ detection of  $\text{Cu}^{2+}$  ions. However absorption titration carried out with all other metal ions showed no significant change, indicating their non-interactive nature with **L** (Fig. 1b). The binding affinities of  $\text{Cu}^{2+}$  toward **L** have also been calculated from the Benesi–Hildebrand equation using absorption data and have been found to have an association constant of  $2.28 \times 10^4 \text{ M}^{-1}$  (Fig. S14A, ESI†).

The chemosensor **L** exhibits weak fluorescence emission at 500 nm owing to the isomerization of the imine C=N bond as well as the excited-state intramolecular proton transfer (ESIPT) from the salicyl -OH to the imine nitrogen when excited at 446 nm in a  $\text{CH}_3\text{CN}-\text{H}_2\text{O}$  mixture (7:3 v/v in 10 mM HEPES

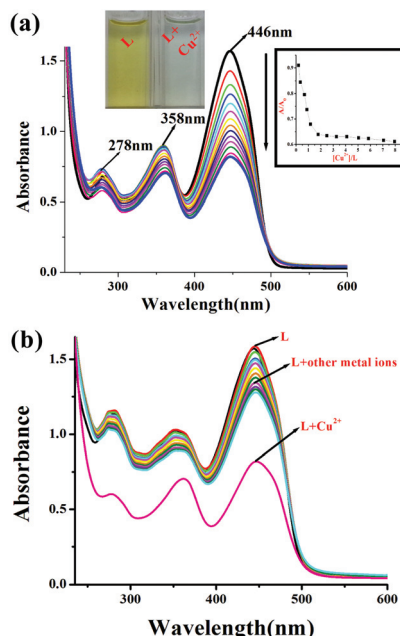


**Fig. 1** (a) UV-vis absorption titration spectra of L ( $c = 4 \times 10^{-5}$  M) in aq. CH<sub>3</sub>CN (CH<sub>3</sub>CN–H<sub>2</sub>O = 7 : 3 v/v, 10 mM HEPES buffer, pH = 7.4) upon addition of Cu<sup>2+</sup> ( $c = 2 \times 10^{-4}$  M). The inset shows the relative absorption intensity ( $A/A_0$ ) as a function of [Cu<sup>2+</sup>]/[L], and the photographs show the color change of L in the presence of Cu<sup>2+</sup>. (b) Competitive absorption spectra of L in the presence of different metal ions (perchlorate, chloride, or nitrate salts of Hg<sup>2+</sup>, Cd<sup>2+</sup>, Fe<sup>2+</sup>, Co<sup>2+</sup>, Ni<sup>2+</sup>, Mn<sup>2+</sup>, Zn<sup>2+</sup>, Au<sup>3+</sup>, Cu<sup>2+</sup>, Ag<sup>+</sup>, Pd<sup>2+</sup>, Cr<sup>3+</sup>, Al<sup>3+</sup>, Pb<sup>2+</sup>, Ca<sup>2+</sup>, Mg<sup>2+</sup>, Na<sup>+</sup>, and K<sup>+</sup>) in aq. CH<sub>3</sub>CN (CH<sub>3</sub>CN–H<sub>2</sub>O = 7 : 3 v/v, 10 mM HEPES buffer, pH = 7.4).

buffer at pH = 7.4) which has been well documented in the literature pertaining to Schiff base molecular systems.<sup>27,28</sup>

The titration of **L** with Cu<sup>2+</sup> results in the enhancement of the fluorescence intensity at 488 nm as a function of [Cu<sup>2+</sup>] (Fig. 2a) and the intensity saturates at >1 equiv. In this connection, it is well known that Cu<sup>2+</sup> is a paramagnetic ion with an unfilled d-shell and could strongly quench the emission of the fluorophore near it *via* electron or energy transfer. But in our case, the enhancement of the emission of **L** after binding of the Cu<sup>2+</sup> ion is quite interesting and mentionable along with the few other related existing systems.<sup>29</sup>

In our opinion, *switch on* fluorescence emission is expected due to the chelation of Cu<sup>2+</sup> through the deprotonated phenolic oxygen, the imine and thiazole N atoms, and the lactone carbonyl oxygen. Such chelation leads to the suppression of C≡N bond isomerization to attain a conjugated coplanar structure as well as ESIPT and fluorescence enhancement takes place as a consequence.<sup>30</sup> Further, chelation imparts rigidity to the system and the metal–fluorophore interaction is modulated, which is the underlying cause of chelation enhanced fluorescence (CHEF).<sup>31</sup>

A plot of the relative fluorescence intensity ( $I/I_0$ ) vs. [Cu<sup>2+</sup>]/[L] mole ratio (Fig. 2a, inset) gives a sigmoidal plot and exhibits a midpoint ratio of 1 : 1 stoichiometric complex for **L** to Cu<sup>2+</sup>. The binding affinities of Cu<sup>2+</sup> toward **L** have been calculated from the Benesi–Hildebrand equation and have been

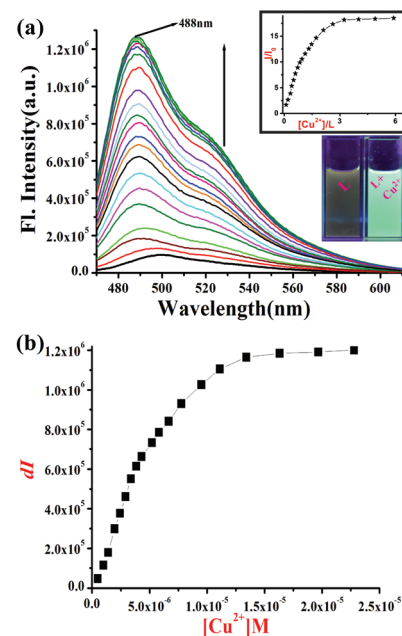


**Fig. 2** (a) Fluorescence emission spectra obtained during the titration of L ( $c = 1 \times 10^{-5}$  M) with Cu<sup>2+</sup> ( $c = 1 \times 10^{-4}$  M) in aqueous CH<sub>3</sub>CN (CH<sub>3</sub>CN–H<sub>2</sub>O = 7 : 3 v/v, 10 mM HEPES buffer, pH = 7.4),  $\lambda_{\text{ext}} = 446$  nm. The inset shows the relative fluorescence intensity ( $I/I_0$ ) as a function of the [Cu<sup>2+</sup>]/[L] mole ratio, and fluorescence emission color changes of the receptor L solution on addition of Cu<sup>2+</sup> ions. (b) Change in emission intensity at 500 nm with incremental addition of Cu<sup>2+</sup> ions [ $\lambda_{\text{ext}} = 446$  nm].

found to have an association constant of  $3.33 \times 10^4$  M<sup>-1</sup> (Fig. S14B, ESI†).

The observed high  $K_a$  value clearly indicates the strong affinity of Cu<sup>2+</sup> toward **L**. The titration of **L** (500 nm) with 3 equiv. Cu<sup>2+</sup> results in a sizable enhancement of fluorescence intensity at 488 nm as a function of the increased Cu<sup>2+</sup> concentration [ $(I_{\text{complex}}/I_{\text{free ligand}}) \sim 18$ -fold] (Fig. 2a). Under UV light, the solution of **L** is weakly fluorescent, whereas in the presence of Cu<sup>2+</sup> an intense green color fluorescence was observed (Fig. 2a, inset) and no such fluorescence color was observed in the case of the other metal ions (Fig. S13, ESI†). Thus, Cu<sup>2+</sup> can easily be differentiated by its fluorescence color change from the other metal ions (Fig. S13, ESI†).

Further, the stoichiometry of the complex formed between **L** and Cu<sup>2+</sup> has been derived to be 1 : 1 based on a Job's plot (Fig. S9, ESI†). The formation of a 1 : 1 binding mode of the sensor with Cu<sup>2+</sup> was also confirmed by ESI-MS, where the spectrum obtained for the *in situ* complex results in a molecular ion peak at  $m/z = 524.7646$  (calc. 524.09) (Fig. S6, ESI†). The mass spectrum is assignable to the mass of  $[L + Cu^{2+} + NH_4^{+}]^+$ , which supports the presence of copper. Therefore, we suggest that probe **L** coordinates with Cu<sup>2+</sup> with a 1 : 1 stoichiometry.

### Competitive metal ion titrations

In order to check the practical utility of Cu<sup>2+</sup> recognition by **L**, competitive titrations were carried out in the presence of other

biologically and ecologically relevant metal ions. Fluorescence spectra (Fig. 3b) were recorded for the titration of **L** against  $\text{Cu}^{2+}$  in the presence of 10 equiv. of other different metal ions, *viz.*  $\text{Au}^{3+}$ ,  $\text{Ag}^+$ ,  $\text{Hg}^{2+}$ ,  $\text{Fe}^{3+}$ ,  $\text{Pd}^{2+}$ ,  $\text{Zn}^{2+}$ ,  $\text{Cd}^{2+}$ ,  $\text{Ni}^{2+}$ ,  $\text{Co}^{2+}$ ,  $\text{Mn}^{2+}$ ,  $\text{Cr}^{3+}$ ,  $\text{Al}^{3+}$ ,  $\text{Pb}^{2+}$ ,  $\text{Ca}^{2+}$ ,  $\text{Mg}^{2+}$ ,  $\text{Na}^+$ , and  $\text{K}^+$ . In the fluorescence titration, the result found, none of these metal ions significantly affect the emission intensity of **L** upon the addition of  $\text{Cu}^{2+}$ , to have only marginal changes in the emission intensity, suggesting that none of these ions interfere in the fluorescence emission of the  $\text{Cu}^{2+}$  complex (Fig. 3b). Therefore, it can be concluded that **L** recognizes  $\text{Cu}^{2+}$  even in the presence of other metal ions. In the other fluorescence titrations that were carried out in the same medium with 17 other different metal ions, *viz.*  $\text{Au}^{3+}$ ,  $\text{Ag}^+$ ,  $\text{Hg}^{2+}$ ,  $\text{Fe}^{3+}$ ,  $\text{Pd}^{2+}$ ,  $\text{Zn}^{2+}$ ,  $\text{Cd}^{2+}$ ,  $\text{Ni}^{2+}$ ,  $\text{Co}^{2+}$ ,  $\text{Mn}^{2+}$ ,  $\text{Cr}^{3+}$ ,  $\text{Al}^{3+}$ ,  $\text{Pb}^{2+}$ ,  $\text{Ca}^{2+}$ ,  $\text{Mg}^{2+}$ ,  $\text{Na}^+$ , and  $\text{K}^+$ , no significant fluorescence enhancement was found except for  $\text{Au}^{3+}$ ,  $\text{Pd}^{2+}$  and  $\text{Zn}^{2+}$  which revealed relatively insignificant fluorescence ON responses in this region, manifesting a pronounced off-on type of  $\text{Cu}^{2+}$  selectivity of **L** (Fig. 3a). Therefore, **L** is selective to  $\text{Cu}^{2+}$  among the 18 ions studied. Visual fluorescence color change experiments have been carried out to look at the behavior of **L** in the presence of various metal ions. A solution of **L** with >1 equiv. of  $\text{Cu}^{2+}$  ions converted the visual emission color from faint yellow to bright green when excited with a handheld 365 nm UV lamp, which is otherwise not present in the

case of the other metal ions studied (Fig. S13, ESI†). Therefore,  $\text{Cu}^{2+}$  can easily be differentiated by visual color change from the other metal ions.

The sensitivity of **L** for  $\text{Cu}^{2+}$  has been further evaluated by measuring the lowest concentration that can be determined. The fluorescence titration carried out between **L** and  $[\text{Cu}^{2+}]$  by maintaining a 1 : 1 ratio gives a value of 1.53  $\mu\text{M}$  suggesting its applicability in the detection of  $\text{Cu}^{2+}$  ions in an aqueous medium under physiological conditions.

To be useful in biological applications, it is necessary for a fluorescent probe to operate over a suitable range of pH values, especially at physiological pH. A series of buffers with pH values ranging from 1 to 13 was prepared by mixing a sodium hydroxide solution and hydrochloric acid in HEPES buffer. Thus, we proceeded to investigate the effect of pH on the fluorescence intensity of the probe **L** in the absence or presence of  $\text{Cu}^{2+}$ . The results showed that the fluorescence intensity ( $I_{488}$  nm) of **L** showed no apparent changes in the pH range from 6.0 to 9.0 no matter with or without  $\text{Cu}^{2+}$ , indicating that **L** is stable in this pH range and its response towards  $\text{Cu}^{2+}$  was also almost invariable in this pH range (Fig. S12, ESI†).

### <sup>1</sup>H NMR titration experiment

To know the mode of complexation of **L** with  $\text{Cu}^{2+}$ , we carried out <sup>1</sup>H NMR titration in  $\text{CDCl}_3$ . During the <sup>1</sup>H NMR titration of **L** with  $\text{Cu}^{2+}$ , the addition of 1 equiv. of  $\text{Cu}^{2+}$  into the solution of **L** in  $\text{CDCl}_3$  provided a very broad <sup>1</sup>H NMR spectrum due to the complexation of paramagnetic  $\text{Cu}^{2+}$  to **L**. The proton NMR signals corresponding to the thiazole ( $\text{H}_c$ ) and imine proton ( $\text{H}_b$ ) experience considerable broadening owing to the binding of this region with paramagnetic  $\text{Cu}^{2+}$  (Fig. 4).

However, treatment of the  $[\text{CuL}]$  system with sulphide ions afforded a well resolved spectrum, which was almost identical with the <sup>1</sup>H NMR spectrum of **L** itself (Fig. S3, ESI†). To further clarify the spectrum, the product of  $[\text{CuL} + \text{S}^{2-}]$  was isolated by a silica gel column and was then subjected to <sup>1</sup>H NMR analysis. The <sup>1</sup>H NMR of the resulting product is essentially identical to that of free **L**.

### Density functional theory (DFT) calculations

To verify the configuration of  $[\text{CuL}]$  and to investigate the electronic structure and electronic transitions of the  $\pi$ -conjugated copper complex, DFT geometry optimizations followed by TD-DFT calculations at the B3LYP level<sup>32</sup> were carried out. All elements except Cu were assigned the 6-31G(d) basis set. The LANL2DZ basis set with an effective core potential (ECP) set of Hay and Wadt<sup>33</sup> was used for Cu. The optimized geometries of **L** and the  $[\text{CuL}]$  complex are shown in (Fig. 5). The complex shows that the  $\text{Cu}^{2+}$  ion binds to **L** very well through four coordination sites, and the whole molecular system forms a nearly planar structure.

The geometry optimizations for **L** and the  $[\text{CuL}]$  complex were done in a cascade fashion starting from semiempirical PM2 followed by *ab initio* HF to DFT B3LYP by using various basis sets, *viz.*, PM2 → HF/STO-3G → HF/3-21G → HF/6-31G →

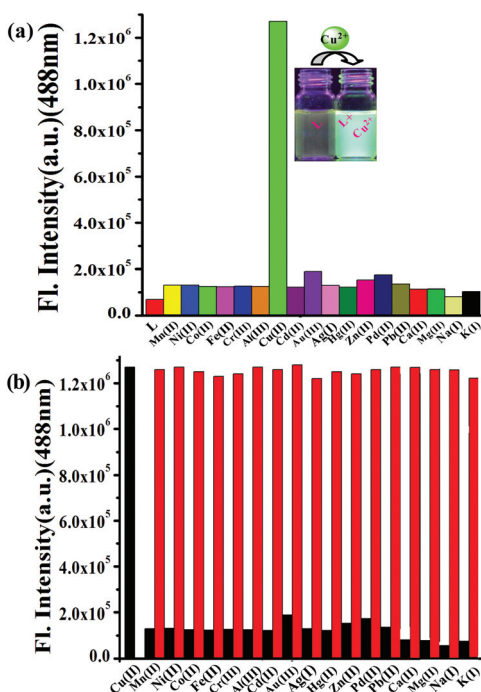


**Fig. 3** (a) Histogram showing the relative fluorescence response of various metal ions ( $c = 1 \times 10^{-4}$  M) with **L** ( $c = 1 \times 10^{-5}$  M) in aq.  $\text{CH}_3\text{CN}$  ( $\text{CH}_3\text{CN}-\text{H}_2\text{O} = 7:3$  v/v, 10 mM HEPES buffer, pH = 7.4). Inset: the fluorescence photograph of **L** and  $\text{L} + \text{Cu}^{2+}$ . (b) Fluorescence response of **L** ( $c = 1 \times 10^{-5}$  M) to addition of 3 equiv.  $\text{Cu}^{2+}$  ( $c = 1 \times 10^{-4}$  M) [the black bar portion] and to the mixture of 10 equiv. of other divalent metal ions with addition of 3 equiv.  $\text{Cu}^{2+}$  [the red bar portion].

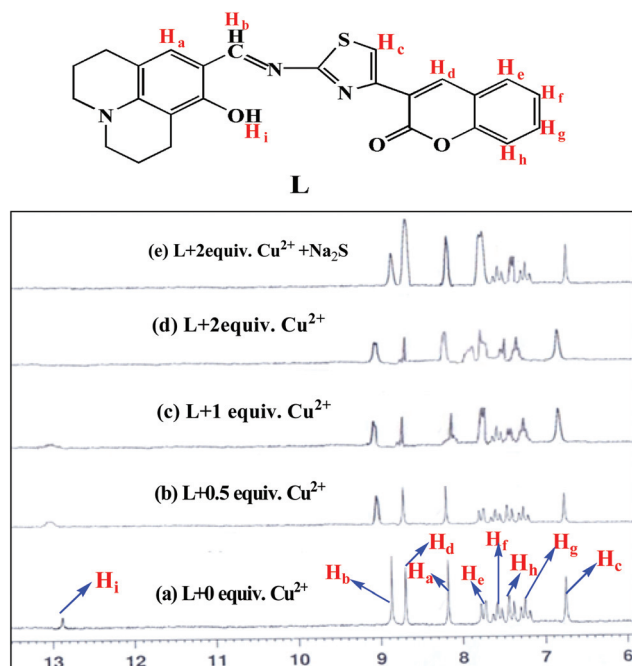


**Fig. 4** Partial  $^1\text{H}$  NMR spectra (400 MHz) of **L** in  $\text{CDCl}_3$  at 25 °C and the corresponding changes after the gradual addition of different equivalents of copper perchlorate in  $\text{MeOH-d}_4$  from (a) **L**, (b) **L** + 0.5 equiv.  $\text{Cu}^{2+}$ , (c) **L** + 1.0 equiv.  $\text{Cu}^{2+}$ , (d) **L** + 2.0 equiv.  $\text{Cu}^{2+}$  and (e) **L** + 2.0 equiv.  $\text{Cu}^{2+}$  +  $\text{Na}_2\text{S}$ .

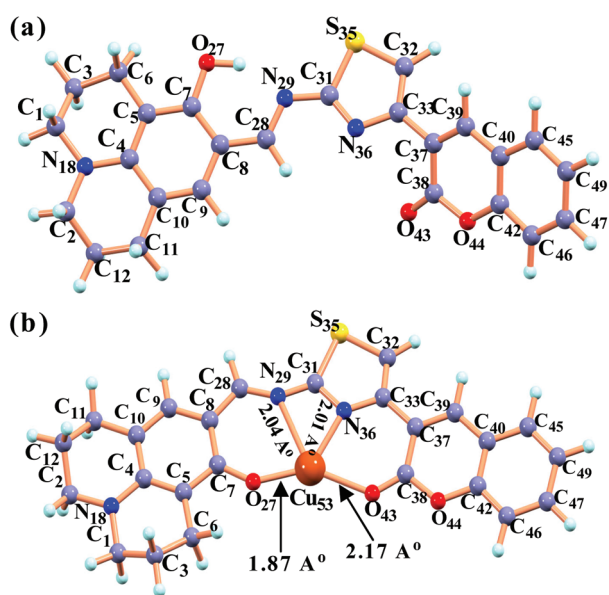


**Fig. 5** B3LYP optimized structure of (a) **L** by the DFT/B3LYP/6-31+G(d) method and (b) **L**- $\text{Cu}^{2+}$  complex by the DFT/UB3LYP method.

B3LYP/6-31G(d,p). For the  $[\text{CuL}]$  complex, a starting model was generated by taking the DFT optimized **L** and placing the  $\text{Cu}^{2+}$  ion well in the core of the coumarin lactonecarbonyl O, enamine N, phenolic OH and/thiazole N as donor moieties at a non-interacting distance. This model was then optimized initially using the HF/3-21G level of calculations, and the

output structure from this was taken as input for DFT calculations performed using B3LYP with a LANL2DZ relativistic pseudopotential basis set for  $\text{Cu}^{2+}$  and 6-31+G(d,p) for all other atoms in the complex.

Geometry optimization resulted in conformational changes at the two sides of the thioimidazole ring, *i.e.*, coumarin and aminophenol parts to accommodate a copper ion. Conformational changes can be estimated through the torsional angles of the two sides (Table S1, ESI<sup>†</sup>) and the structure is given in Fig. 5. In the process, the lactone oxygen of the coumarin moiety and the phenolate oxygen of the aminophenol part turned in the same direction to form a binding core. In the  $[\text{CuL}]$  optimized structure, the copper is bound by two nitrogen atoms (imine and thioimidazole) and two oxygen atoms (coumarin lactone and phenolate oxygens) in the binding core ( $\text{N}_2\text{O}_2$ ) leading to highly distorted geometries about the copper centers that deviate from both the tetrahedral as well as the square planar.

The optimized complex of  $\text{Cu}^{2+}$  with **L** associated with four bonds ( $\text{N}_{29}-\text{Cu}$ ,  $\text{N}_{36}-\text{Cu}$ ,  $\text{O}_{43}-\text{Cu}$  and  $\text{O}_{27}-\text{Cu}$ ) to the central ion with their distances being 2.04, 2.01, 2.17 and 1.87 Å respectively (Table S1, ESI<sup>†</sup>).<sup>33</sup> The geometry about  $\text{Cu}^{2+}$  is significantly distorted exhibiting coordination angles in the range of 65.59–120.97°. The spatial distributions and orbital energies of the HOMO and LUMO of **L** and  $[\text{CuL}]$  were also determined (Fig. 6a).

The  $\pi$  electrons on the relevant HOMOs and LUMOs of the  $[\text{CuL}]$  complex are essentially distributed in the entire coumarinthioimidazole-aminophenol backbone. By contrast, in the case of **L**, the  $\pi$  electrons on HOMO and HOMO-1 primarily reside on the electron-donating aminophenol moiety, whereas those on LUMO, HOMO-2 and LUMO+2 are mainly located on the electron withdrawing coumarin moiety (Fig. 6b). This indicates that **L** bears efficient electron transfer from the aminophenol moiety to the coumarin parts, thus rendering the fluorescence relatively weak ( $\phi = 0.020$ ). By contrast, the nearly complete overlap of electrons on the transition orbitals may induce a strong fluorescence emission for the  $[\text{CuL}]$  complex ( $\phi = 0.62$ ).<sup>34</sup> Moreover, the HOMO-LUMO energy gap of the complex becomes much smaller relative to that of probe **L**. The energy gaps between HOMO and LUMO in the probe **L** and the  $[\text{CuL}]$  complex were 3.23 eV and 2.88 eV respectively (Fig. 6a).

### SEM imaging studies

To understand the aggregation property of **L** and  $[\text{CuL}]$ , and its effect on their chemo-sensing property, scanning electron microscope (SEM) imaging was carried out. **L** and  $[\text{CuL}]$  possess charge transfer, hydrogen bonding,  $\pi$ - $\pi$  stacking, and van der Waals force of attraction which cause the compounds to form a sheet-like 2D nanostructure and globular material respectively (Fig. 7a and b). The exact aggregation mechanism to construct uniform globular material is unknown to us. However, in the presence of a  $\text{Cu}^{2+}$ -ion a strong complexation with the ligand along with charge transfer is expected. This

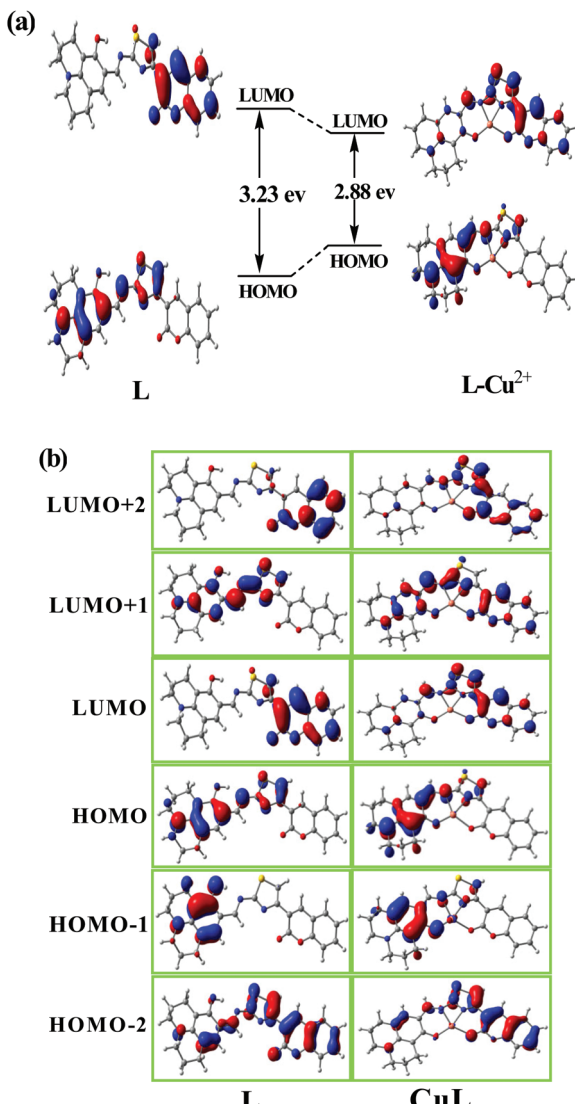


**Fig. 6** (a) HOMO and LUMO distributions of L and the L–Cu<sup>2+</sup> complex. (b) Molecular orbital plots of L and L–Cu<sup>2+</sup>.

SEM imaging study supports the unprecedented chemosensing nature of L and [CuL] which can be utilized for cell imaging.

#### Fluorescence and UV-Vis spectroscopic studies of the [CuL] complex in the presence of S<sup>2-</sup>

Since L detects Cu<sup>2+</sup> selectively, the *in situ* prepared [CuL] complex has been used for anion recognition studies. Owing to the strong affinity of Cu<sup>2+</sup> towards sulphide the highly fluorescent [CuL] complex has been studied for its secondary sensing property toward a selective anion.<sup>35</sup> The chemosensing ensemble was prepared *in situ* by mixing L and Cu<sup>2+</sup> in a 1 : 1 ratio and it has been used for anion recognition studies for different anions, *viz.*, F<sup>-</sup>, Br<sup>-</sup>, S<sup>2-</sup>, I<sup>-</sup>, CN<sup>-</sup>, SO<sub>4</sub><sup>2-</sup>, SCN<sup>-</sup>, AcO<sup>-</sup>, Cl<sup>-</sup>, H<sub>2</sub>PO<sub>4</sub><sup>-</sup>, PO<sub>4</sub><sup>3-</sup>, NO<sub>3</sub><sup>-</sup>, ClO<sub>4</sub><sup>-</sup> and HSO<sub>4</sub><sup>-</sup>. All anion titrations exhibited no significant change in the fluorescence intensity except sulphide and cyanide.

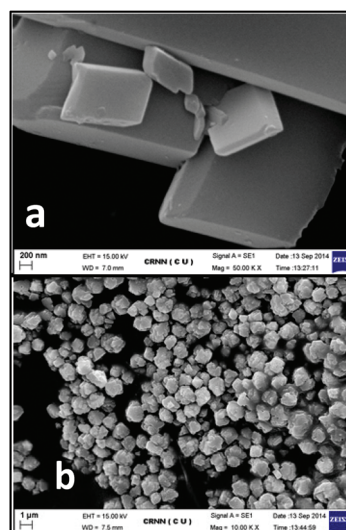


**Fig. 7** (a) Monolayer SEM image of L and (b) SEM image of the L–Cu<sup>2+</sup> complex.

During the titration of [CuL] with sulphide, the emission band observed at 488 nm is quenched (Fig. 8a) gradually to reach an intensity that is similar to that of L. This is exactly the reverse of what happens when L is titrated with Cu<sup>2+</sup>, indicating the removal of Cu<sup>2+</sup> by sulphide and thereby releasing the free L. This is true even with cyanide (Fig. S16, ESI†) (Fig. 9).

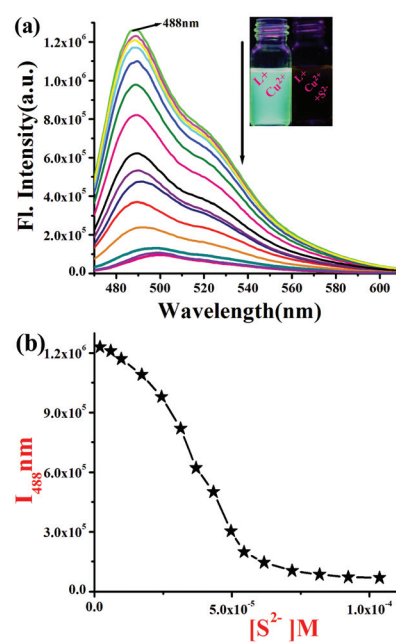


**Fig. 8** (a) Fluorescence spectra of L ( $c = 1 \times 10^{-5}$  M) with 3 equiv. of Cu<sup>2+</sup> upon addition of sodium sulphide ( $c = 4 \times 10^{-4}$  M) in aq. CH<sub>3</sub>CN (CH<sub>3</sub>CN-H<sub>2</sub>O = 7 : 3 v/v, 10 mM HEPES buffer, pH = 7.4) and photographs of L + Cu<sup>2+</sup>, L + Cu<sup>2+</sup> + S<sup>2-</sup> in color changes. (b) Fluorescence intensity ( $I$ ) vs. [S<sup>2-</sup>] mole ratio plot at 488 nm, [ $\lambda_{\text{ext}} = 446$  nm].

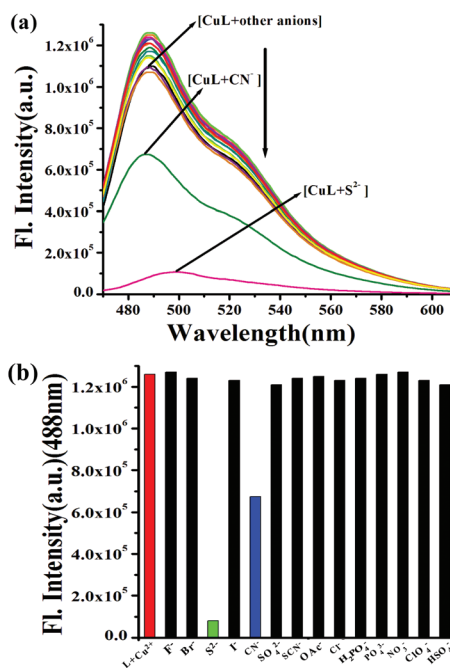


**Fig. 9** (a) Competitive fluorescence spectra of CuL ( $1.0 \times 10^{-5}$  M) in the presence of tetrabutyl ammonium salt of different anions ( $4.0 \times 10^{-4}$  M) ( $F^-$ ,  $Br^-$ ,  $S^{2-}$ ,  $I^-$ ,  $CN^-$ ,  $SO_4^{2-}$ ,  $SCN^-$ ,  $AcO^-$ ,  $Cl^-$ ,  $H_2PO_4^-$ ,  $PO_4^{3-}$ ,  $NO_3^-$ ,  $ClO_4^-$  and  $HSO_4^-$ ) in  $CH_3CN-H_2O$  (7 : 3 v/v, pH = 7.4). (b) The anion sensitivity profile for CuL: the change in the emission intensity of CuL ( $1.0 \times 10^{-5}$  M) in the presence of 4.5 equivalents of  $S^{2-}$  ion, and 10 equivalents of other interfering anions in aq.  $CH_3CN$  ( $CH_3CN-H_2O$  = 7 : 3 v/v, 10 mM HEPES buffer, pH = 7.4).

Thus the [CuL] complex acts as a secondary recognition ensemble toward sulphide, and cyanide. The minimum concentration of sulphide that can be detected by [CuL] has been found to be 11.4  $\mu$ M (Fig. S15B, ESI†).

In order to support the results obtained from the fluorescence studies by effecting the removal of  $Cu^{2+}$  by sulphide ion, similar absorption titrations were carried out. During the titration of [CuL] by  $CN^-$  (Fig. 10a), the low energy absorption band arising from the precursor complex observed at 446 nm progressively increases and a gradual addition of sulphide produces two bands, one at 278 nm and the other at 358 nm, which correspond to the free receptor L, and the absorbance of these bands increases (Fig. 10a).

All these suggest the disruption of the [CuL] complex followed by the removal of  $Cu^{2+}$  by the sulphide as well as cyanide ions to result in a free receptor. It has been noted that the changes observed for different bands during titration between [CuL] and  $S^{2-}$  are exactly the reverse of those observed during the titration of L with  $Cu^{2+}$  (Fig. 1a). This suggests a displacement mechanism during the titration of  $S^{2-}$ . Similar observations were noticed with  $CN^-$ . Sulphide selective signalling was not affected by the presence of other common interfering anions. Competition experiments of the [CuL] system revealed that the  $S^{2-}$  induced fluorescence turn-off was retained in the presence of 100 equiv. of other common, co-

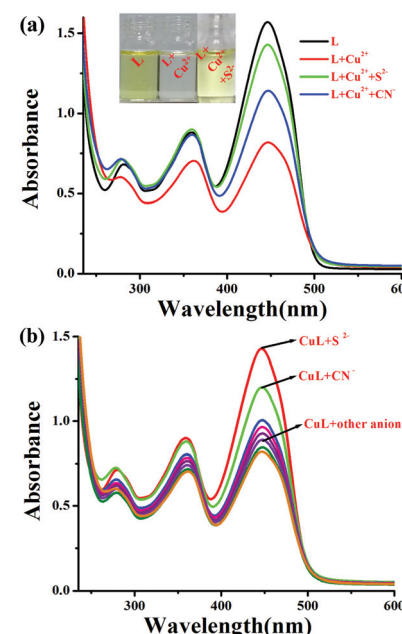


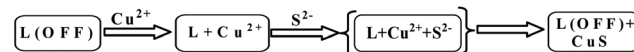
**Fig. 10** (a) Changes in the absorption spectra of the L-Cu complex ( $1.0 \times 10^{-5}$  M) in the presence of  $S^{2-}$ ,  $CN^-$  ( $4.0 \times 10^{-4}$  M) in aq.  $CH_3CN$  ( $CH_3CN-H_2O$  = 7 : 3 v/v, 10 mM HEPES buffer, pH = 7.4). (b) Competitive UV-vis titration spectra of CuL ( $1.0 \times 10^{-5}$  M) in the presence of tetrabutyl ammonium salt of different anions ( $4.0 \times 10^{-4}$  M) ( $F^-$ ,  $Br^-$ ,  $S^{2-}$ ,  $I^-$ ,  $CN^-$ ,  $SO_4^{2-}$ ,  $SCN^-$ ,  $AcO^-$ ,  $Cl^-$ ,  $H_2PO_4^-$ ,  $PO_4^{3-}$ ,  $NO_3^-$ ,  $ClO_4^-$  and  $HSO_4^-$ ) in  $CH_3CN-H_2O$  (7 : 3 v/v, pH = 7.4).

existing anions. Thus, the ensemble seems to be useful for selectively sensing  $S^{2-}$  even involving relevant anions.

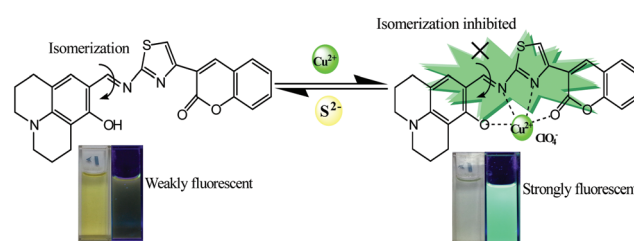
#### Reusability and reversibility of the receptor L

Reversibility is an important aspect of any receptor to be employed as a chemical sensor for detection of specific metal ions. To examine whether the process was reversible, an excess amount of  $S^{2-}$  was added into a solution of the [CuL] ensemble (Schemes 2 and 3).

The bright green fluorescence immediately turned off (Fig. 8a, inset). The reusability of [CuL] in sensing  $S^{2-}$  has



**Scheme 2** Schematic presentation for fluorescence quenching.



**Scheme 3** Proposed mechanism for the fluorescence changes of L upon addition of  $Cu^{2+}$ .

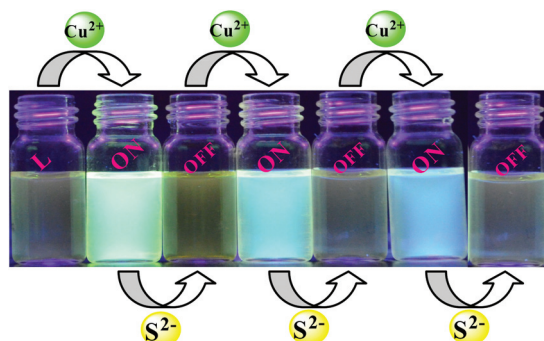


**Fig. 11** Fluorescence experiment showing on-off reversible visual fluorescence color changes after each addition of  $\text{Cu}^{2+}$  and  $\text{S}^{2-}$  sequentially.

been demonstrated by carrying out four alternate cycles of titration of  $[\text{CuL}]$  with  $\text{S}^{2-}$  followed by  $\text{Cu}^{2+}$ . The titration of  $[\text{CuL}]$  with  $\text{S}^{2-}$  shows a significant switch off fluorescence, and the fluorescence is regained when  $\text{Cu}^{2+}$  is added to result in a switch on mode. Three such consecutive cycles are shown in Fig. 11, and the results clearly demonstrate the reversible property of **L** in sensing  $\text{Cu}^{2+}$  followed by  $\text{S}^{2-}/\text{CN}^-$  (Fig. S16, ESI†).

### Detection and imaging in living cells

The desirable features of chemosensor **L** such as high sensitivity with a turn-on fluorescence, fast response, reversibility, good performance at physiological pH, and high selectivity encouraged us to further evaluate the potential of the sensor for imaging  $\text{Cu}^{2+}$  in living cells. Here Vero cells (very thin endothelial cell) were used as models (Experimental section). Before microscopic imaging, all the solutions were aspirated and mounted on slides in a mounting medium containing DAPI ( $1 \mu\text{g mL}^{-1}$ ) to label the cell nuclei and stored in dark before microscopic images were acquired. Vero cells incubated with only sensor **L** ( $1 \mu\text{M}$ ) exhibited very weak intracellular fluorescence. Again, the cells were pre-treated with  $\text{Cu}^{2+}$  in the growth medium for 30 min. The cells were then washed with PBS to remove the remaining  $\text{Cu}^{2+}$  and further incubated with probe **L** for 30 min.

Vero cells incubated with chemosensor **L** exhibited very weak fluorescence, whereas a bright green fluorescence signal was observed in the cells stained with both the chemosensor **L** and  $\text{Cu}^{2+}$ , which in good agreement with the fluorescence turn-on profile of the sensor in the presence of  $\text{Cu}^{2+}$  in the solution (Fig. 12[E–H]). Moreover, bright green colored fluorescence cells obtained from the incubation of the receptor **L** followed by treatment with  $\text{Cu}^{2+}$  became invisible in fluorescence upon addition of  $\text{Na}_2\text{S}$  ( $40 \mu\text{M}$ ) (Fig. 12[I–L]). The results establish that sensor **L** is cell membrane permeable and capable of sensing  $\text{Cu}^{2+}$  in living cells. To the best of our knowledge, this is the first known thiazole-coumarin-based conjugate in the literature which has been demonstrated to recognize  $\text{Cu}^{2+}$  in live cells. Cells were intact and showed a healthy spread and adherent morphology during and after the

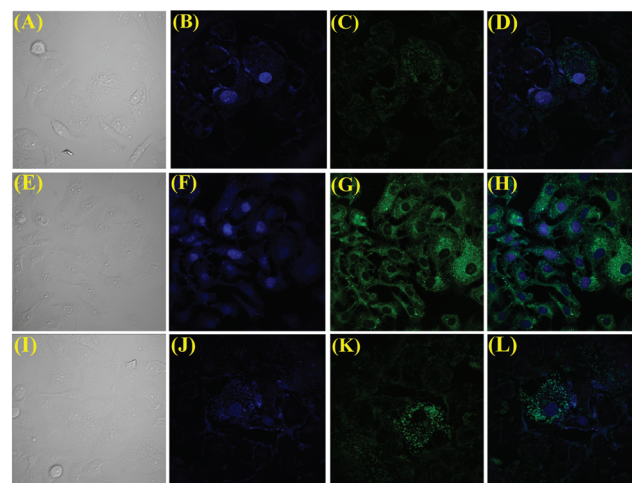


**Fig. 12** Confocal microscopic images of probe in Vero 76 cells pre-treated with  $\text{Cu}^{2+}$ : (A) bright field image of the cells of controlled set. (B) Only  $\text{Cu}^{2+}$  at  $1.0 \times 10^{-4} \text{ M}$  concentration, nuclei counterstained with DAPI ( $1 \mu\text{g mL}^{-1}$ ). (C) Only  $\text{Cu}^{2+}$  at  $1.0 \times 10^{-4} \text{ M}$  concentration. (D) Overlay of (B) and (C). (E) Bright field image of the cells stained with probe **L** at a concentration  $1.0 \times 10^{-6} \text{ M}$ . (F) Image scan of DAPI for E. (G) With probe **L** at a concentration of  $1.0 \times 10^{-6} \text{ M}$  detected on  $\lambda_{\text{ext}} = 450 \text{ nm}$ ,  $\lambda_{\text{em}} = 519 \text{ nm}$ . (H) Overlaid image of F and G. (I) Bright field image of the cells treated with  $1.0 \times 10^{-4} \text{ M Cu}^{2+}$ ,  $1.0 \times 10^{-6} \text{ M}$  probe **L** and  $\text{Na}_2\text{S}$  at a concentration of  $4.0 \times 10^{-5} \text{ M}$ . (J) Cells of I scanned for DAPI. (K) Cells of I scanned at  $\lambda_{\text{ext}} = 473$ ,  $\lambda_{\text{em}} = 519$ . (L) Overlay of J and K. All images were acquired with a  $60\times$  objective lens. Scale bar represents  $20 \mu\text{m}$ .

labeling process with chemosensor **L**, indicating absence of cytotoxic effects.

### Conclusion

The iminothioimidazole-phenolic-coumarin based probe **L** was synthesized and characterized. It was found to be a sensitive and selective fluoroionophore of  $\text{Cu}^{2+}$  among the eighteen different metal ions studied in HEPES buffer medium. The selectivity and sensitivity were demonstrated on the basis of fluorescence, absorption, and  $^1\text{H}$  NMR spectroscopy, ESI mass spectrometry, and visual fluorescence color changes. The interaction of  $\text{Cu}^{2+}$  with **L** enhances the fluorescence emission and induces a turn on response in the electronic and fluorescence spectra in the visible region. Thus, these receptors can be used as dual probes for visual detection through change in color and fluorescence. Fluorescence and absorption spectroscopy provide information about the formation of a  $1:1$  complex between  $\text{Cu}^{2+}$  and **L**, and ESI-MS confirms the fact. The association constant,  $K_a$  for **L** with  $\text{Cu}^{2+}$  is in the order of  $10^4 \text{ M}^{-1}$  based on fluorescence as well as absorption studies, suggesting a strong binding for  $\text{Cu}^{2+}$ . The receptor **L** has been shown to be sensitive with a minimum detection limit of  $1.53 \mu\text{M} \pm 0.1 \text{ ppm Cu}^{2+}$ . The  $\text{Cu}^{2+}$  binding characteristics of **L** have been studied by computational calculations at the DFT level and TDDFT calculations were carried out to demonstrate the

electronic properties of **L** and the corresponding copper complex. The *in situ* prepared copper complex of **L**, *viz.*, **L-Cu**, was able to detect S<sup>2-</sup> in a manner exactly reverse of what happens when Cu<sup>2+</sup> is added to **L** in fluorescence spectroscopy. To know the supramolecular microstructural features of **L** and the **L-Cu** complex, SEM studies were carried out in which the spherically shaped particles of **L** were found enlarged as well as aggregated in the complex. Nonfluorescence images were observed when Vero cells were incubated with probe **L** alone. However, strong green fluorescence was observed in Vero cells in the presence of Cu<sup>2+</sup>. Hence, these results clearly indicate that probe **L** is an effective intracellular Cu<sup>2+</sup> imaging agent with cell permeability.

## Experimental section

### General information and materials

All the solvents were of analytic grade. All cationic compounds such as perchlorates of Hg<sup>2+</sup>, Cd<sup>2+</sup>, Fe<sup>2+</sup>, Co<sup>2+</sup>, Ni<sup>2+</sup>, Mn<sup>2+</sup>, Zn<sup>2+</sup>, Au<sup>3+</sup>, Cu(ClO<sub>4</sub>)<sub>2</sub>, nitrates of Ag<sup>+</sup>, Pb<sup>2+</sup>, chlorides of Cr<sup>3+</sup>, Al<sup>3+</sup>, and Pb<sup>2+</sup> were purchased from Sigma-Aldrich Chemical Co., stored in a desiccator under vacuum containing self-indicating silica, and used without any further purification. Solvents were dried according to standard procedures. Unless stated otherwise, commercial grade chemicals were used without further purification. Elix Millipore water was used throughout all experiments. All reactions were magnetically stirred and monitored by thin-layer chromatography (TLC) using Spectrochem GF254 silica gel coated plates. Column chromatography was performed with activated neutral aluminum oxide. FTIR spectra were recorded as KBr pellets using a JASCO FTIR spectrometer (model FTIR-460 plus). The <sup>1</sup>H NMR spectra were recorded on a Bruker 400 MHz spectrometer. Mass spectra were recorded using a Waters QTOF Micro YA 263 mass spectrometer. The <sup>1</sup>H NMR chemical shift values are expressed in ppm ( $\delta$ ) relative to CHCl<sub>3</sub> ( $\delta$  = 7.26 ppm). UV-vis and fluorescence spectra measurements were performed on a JASCO V530 and a Photon Technology International (PTI-LPS-220B) spectrofluorimeter, respectively. The following abbreviations are used to describe spin multiplicities in <sup>1</sup>H NMR spectra: s = singlet; d = doublet; t = triplet; m = multiplet.

### Synthesis and characterization of **L**

Synthesis of (2): a mixture of compound 1 (3-bromoacetyl coumarin) (0.50 g, 1.87 mmol) and thiourea (0.168 g, 2.21 mmol) in 15 ml absolute ethanol was refluxed for 12 h. After the completion of the reaction (monitored by TLC) the solvent was evaporated and the reaction mixture was poured into ice-water, and the powdered product was extracted with CHCl<sub>3</sub>. The organic layer was washed with a saturated aqueous solution of NaCl, dried over anhydrous MgSO<sub>4</sub> and evaporated to give a yellow solid which was crystallized from the MeOH-CHCl<sub>3</sub> (1 : 1) solution to give compound 2 in 69% yield; M.P. > 250 °C. <sup>1</sup>H NMR (400 MHz, d<sub>6</sub>-DMSO, Si(CH<sub>3</sub>)<sub>4</sub>, *J* (Hz),  $\delta$  (ppm)): 8.50 (1H, s), 7.83 (1H, d, *J* = 7.76 Hz), 7.60 (1H, t, *J* = 7.82 Hz), 7.50

(1H, s), 7.43 (1H, d, *J* = 8.28 Hz), 7.37 (1H, t, *J* = 7.52 Hz), 7.16 (2H, s). TOF MS ES<sup>+</sup>, *m/z* = 245.0093, [M + H]<sup>+</sup>, calc. for C<sub>12</sub>H<sub>8</sub>N<sub>2</sub>O<sub>2</sub>S = 244.26.

### Synthesis of chemosensor **L**

To a mixture of compound 2 (0.112 g, 0.4608 mmol) and 2,3,6,7-tetrahydro-1*H*,5*H*-benzo[*ij*]quinolizine-9-carboxaldehyde (3) (0.10 g, 0.4608 mmol) in dry EtOH (10 ml) 2–3 drops of AcOH were added; then the reaction mixture was refluxed for 4–6 hours. After the completion of the reaction the solvent was evaporated and the deep yellow solid precipitated was filtered through suction, washed with Millipore water and thereafter washed several times with EtOH and dried in air. The deep yellow compound **L** was collected in 72% yield; M.P. > 250 °C. <sup>1</sup>H NMR (CDCl<sub>3</sub>, 400 MHz)  $\delta$  (ppm): 12.91 (1H, s, -OH), 8.84 (1H, s, -CH=N), 8.72 (1H, s), 8.20 (1H, s), 7.63 (1H, d, *J* = 6.8 Hz), 7.52 (1H, t, *J* = 7.2 Hz), 7.36 (1H, d, *J* = 8.2 Hz), 7.30 (1H, t, *J* = 7.7 Hz), 6.85 (1H, s), 3.31–3.26 (4H, q, *J* = 8 Hz), 2.75–2.68 (4H, m), 1.95 (4H, t, *J* = 5.6). <sup>13</sup>C NMR (CDCl<sub>3</sub>, 500 MHz)  $\delta$  (ppm): 19.2, 19.9, 20.9, 21.8, 26.4, 31.1, 33.0, 49.1, 49.4, 105.2, 107.0, 113.2, 113.3, 115.5, 116.1, 118.8, 120.2, 123.7, 127.5, 130.5, 138.4, 144.7, 147.7, 152.1, 162.2; LCMS ES<sup>+</sup>, *m/z* = 444.2, [M + H]<sup>+</sup>, calc. for C<sub>25</sub>H<sub>21</sub>N<sub>3</sub>O<sub>3</sub>S = 443.13.

### UV-vis spectral studies

A stock solution of the probe **L** ( $4.0 \times 10^{-5}$  M) was prepared in CH<sub>3</sub>CN-H<sub>2</sub>O (7 : 3 v/v). Solutions of  $2.0 \times 10^{-4}$  M salts of the respective cations were prepared in Millipore water. All experiments were carried out in a CH<sub>3</sub>CN-H<sub>2</sub>O solution (CH<sub>3</sub>CN-H<sub>2</sub>O = 7 : 3 v/v, 10 mM HEPES buffer, pH = 7.4). In titration experiments, each time a  $4 \times 10^{-5}$  M solution of **L** was filled in a quartz optical cell of 1 cm optical path length, and ion stock solutions were added into the quartz optical cell gradually by using a micropipette. Spectral data were recorded at 1 min after the addition of the ions. In selectivity experiments, the test samples were prepared by placing appropriate amounts of the anion/cation stock into 2 mL of a solution of **L** ( $4 \times 10^{-5}$  M).

### Fluorescence spectral studies

A stock solution of the probe **L** ( $1.0 \times 10^{-5}$  M) was prepared in CH<sub>3</sub>CN-H<sub>2</sub>O (7 : 3 v/v). Solutions of  $1.0 \times 10^{-4}$  M salts of the respective cations were prepared in Millipore water. All experiments were carried out in a CH<sub>3</sub>CN-H<sub>2</sub>O solution (CH<sub>3</sub>CN-H<sub>2</sub>O = 7 : 3 v/v, 10 mM HEPES buffer, pH = 7.4). In titration experiments, each time a  $1 \times 10^{-5}$  M solution of **L** was filled in a quartz optical cell of 1 cm optical path length, and ion stock solutions were added into the quartz optical cell gradually by using a micropipette. Spectral data were recorded at 1 min after the addition of the ions. In selectivity experiments, the test samples were prepared by placing appropriate amounts of the anion/cation stock into 2 mL of a solution of **L** ( $1 \times 10^{-5}$  M). For fluorescence measurements, excitation was provided at 446 nm, and emission was collected from 470 to 610 nm.

## Finding the detection limit

The detection limit was calculated on the basis of the fluorescence titration (Fig. S13, ESI†). The fluorescence emission spectrum of **L** was measured 10 times, and the standard deviation of blank measurement was achieved. To obtain the slope, the ratio of the fluorescence intensity at 488 nm was plotted as a concentration of  $\text{Cu}^{2+}$ . So the detection limit was calculated with the following equation:

$$\text{Detection limit} = 3\text{Sb1}/S \quad (1)$$

where  $\text{Sb1}$  is the standard deviation of the blank measurement and  $S$  is the slope of the calibration curve.

## Computational studies

All geometries for **L** and  $\text{L-Cu}^{2+}$  were optimized by density functional theory (DFT); calculations were performed with the Gaussian09 program package,<sup>36</sup> with the aid of the GaussView visualization program.

## Cell line and cell culture

Vero cell (very thin endothelial cell) (Vero 76, ATCC no. CRL-1587) lines were prepared from continuous culture in Dulbecco's modified Eagle's medium (DMEM, Sigma Chemical Co., St. Louis, MO) supplemented with 10% fetal bovine serum (Invitrogen), penicillin ( $100 \mu\text{g mL}^{-1}$ ), and streptomycin ( $100 \mu\text{g mL}^{-1}$ ). The Vero 76 were obtained from the American Type Culture Collection (Rockville, MD) and maintained in DMEM containing 10% (v/v) fetal bovine serum and antibiotics in a  $\text{CO}_2$  incubator. Cells were initially propagated in  $75 \text{ cm}^2$  polystyrene, filter-capped tissue culture flask under an atmosphere of 5%  $\text{CO}_2$  and 95% air at 37 °C in a  $\text{CO}_2$  incubator. When the cells reached the logarithmic phase, the cell density was adjusted to  $1.0 \times 10^5$  per well in the culture media. The cells were then inoculated in a glass bottom dish, with 1.0 mL ( $1.0 \times 10^4$  cells) of cell suspension in each dish. After cell adhesion, the culture medium was removed. The cell layer was rinsed twice with phosphate buffered saline (PBS), and then treated according to the experimental need.

## Cell imaging study

For confocal imaging studies Vero cells,  $1 \times 10^4$  cells in 1000  $\mu\text{L}$  of the medium, were seeded on a sterile 35 mm covered Petri dish, glass bottom culture dish (ibidi GmbH, Germany), and incubated at 37 °C in a  $\text{CO}_2$  incubator for 10 hours. Then they were washed with 500  $\mu\text{L}$  DMEM followed by incubation with  $1.0 \times 10^{-4} \text{ M Cu}(\text{ClO}_4)_2$  dissolved in 500  $\mu\text{L}$  DMEM at 37 °C for 1 h in a  $\text{CO}_2$  incubator and observed under an Olympus IX81 microscope equipped with a FV1000 confocal system using 1003 oil immersion Plan Apo (N.A. 1.45) objectives. Images obtained through section scanning were analyzed using Olympus Fluoview (version 3.1a; Tokyo, Japan) with excitation with a 446 nm monochromatic laser beam, and emission spectra were integrated over the range of 470–600 nm (single channel). The cells were again washed thrice with phosphate buffered saline (PBS) (pH 7.4) to remove any free Cu-

$(\text{ClO}_4)_2$  and incubated in PBS containing probe **L** to a final concentration of  $1.0 \times 10^{-6} \text{ M}$ , and incubated for 10 min followed by washing with PBS three times to remove excess probe outside the cells and then images were captured. In a separate culture dish undergoing the same treatment the cells were then treated with  $4.0 \times 10^{-5} \text{ M}$  of an  $\text{Na}_2\text{S}$  solution for 1 h; the cells were washed with PBS three times to remove free compounds and ions before analysis. In a separate culture dish the cells were similarly treated with  $1.0 \times 10^{-6} \text{ M}$  probe **L**, incubated for 10 min, washed thrice with PBS and the image was captured to obtain any possible background fluorescence. According to the need of the experiment we follow similar procedures to label the cell nuclei by treatment with DAPI ( $1 \mu\text{g mL}^{-1}$ ) followed by washing three times with PBS and subsequently the image was captured with the excitation wavelength of the laser being 473 nm, and emission being 519 nm. For all images, the confocal microscope settings, such as transmission density, and scan speed, were kept constant to compare the relative intensity of intracellular fluorescence. Before microscopic imaging, all the solutions were aspirated and mounted on slides in a mounting medium containing DAPI ( $1 \mu\text{g mL}^{-1}$ ) to label the cell nuclei and stored in the dark before microscopic images were acquired.

## Cytotoxicity assay

The cytotoxic effects of probe **L**,  $\text{Cu}(\text{ClO}_4)_2$ , and the  $\text{L-Cu}^{2+}$  complex were determined by the MTT [3-(4,5-dimethylthiazol-2-yl)-2,5-diphenyltetrazolium bromide] assay following the manufacturer's instructions (MTT 2003, Sigma-Aldrich, MO). Vero cells were cultured into 96-well plates ( $10^4$  cells per well) for 24 h. After overnight incubation, the medium was removed, and various concentrations of **L**,  $\text{Cu}(\text{ClO}_4)_2$ , and  $\text{L-Cu}^{2+}$  complex (0, 5, 25, 50, 75, and 100  $\mu\text{M}$ ) made in DMEM were added to the cells and incubated for 24 h. Control experiments were set with DMSO; cells without any treatment and cell-free medium were also included in the study. Following incubation, the growth medium was removed, and fresh DMEM containing MTT solution was added. The plate was incubated for 3–4 h at 37 °C. Subsequently, the supernatant was removed, and the insoluble colored formazan product was solubilized in DMSO, and its absorbance was measured using a microplate reader (Perkin-Elmer) at 570 nm. The assay was performed in triplicate for each concentration of **L**,  $\text{Cu}(\text{ClO}_4)_2$ , and  $\text{L-Cu}^{2+}$ . The OD value of wells containing only DMEM medium was subtracted from all readings to get rid of background influence. Cell viability was calculated by the following formula: (mean OD in treated wells/mean OD in control wells)  $\times 100$ .

## Acknowledgements

We thank the DST-West Bengal [Project no. 124(Sanc.)/ST/P/S&T/9G-17/2012] for financial support. SM and SKM thank the UGC, New Delhi for a fellowship.

## Notes and references

- 1 A. Mathie, G. L. Sutton, C. E. Clarke and E. L. Veale, *Pharm. Ther.*, 2006, **111**, 567.
- 2 J. Stöckel, J. Safar, A. C. Wallace, F. E. Cohen and S. B. Prusiner, *Biochemistry*, 1998, **37**, 7185.
- 3 B. Halliwell and J. M. C. Gutteridge, *Biochem. J.*, 1984, **219**, 1.
- 4 P. C. Bull, G. R. Thomas, J. M. Rommens, J. R. Forbes and D. W. Cox, *Nat. Genet.*, 1993, **5**, 327.
- 5 J. S. Valentine and P. J. Hart, *Proc. Natl. Acad. Sci. U. S. A.*, 2003, **100**, 3617.
- 6 C. Vulpe, B. Levinson, S. Whitney, S. Packman and J. Gitschier, *Nat. Genet.*, 1993, **3**, 7.
- 7 Y. H. Hung, A. I. Bush and R. A. Cherny, *J. Biol. Inorg. Chem.*, 2010, **15**, 61.
- 8 M. C. Linder and M. Hazegh-Azam, *Am. J. Clin. Nutr.*, 1996, **63**, 797S.
- 9 R. Uauy, M. Olivares and M. Gonzalez, *Am. J. Clin. Nutr.*, 1998, **67**, 952S.
- 10 (a) M. Y. Pamukoglu and F. Kargi, *J. Hazard. Mater.*, 2007, **148**, 2744; (b) P. G. Welsh, J. Lipton, C. A. Mebane and J. C. A. Marr, *Ecotoxicol. Environ. Saf.*, 2008, **69**, 199; (c) K. N. Buck, J. R. M. Ross, A. R. Flegal and K. W. Bruland, *Environ. Res.*, 2007, **105**, 5; (d) E. Van Genderen, R. Gensemer, C. Smith, R. Santore and A. Ryan, *Aquat. Toxicol.*, 2007, **84**, 279; (e) P. Kumar, R. K. Tewari and P. N. Sharma, *Plant Cell Rep.*, 2008, **27**, 399.
- 11 A. P. de Silva, H. Q. N. Gunarante, T. Gunnlaugsson, A. J. M. Huxley, C. P. McCoy, J. T. Rademacher and T. E. Rice, *Chem. Rev.*, 1997, **97**, 1515.
- 12 (a) Q. Zeng, P. Cai, Z. Li, J. Qin and B. Z. Tang, *Chem. Commun.*, 2008, 1094; (b) J. Xie, M. Méenand, S. Maisonneuve and R. Méétivier, *J. Org. Chem.*, 2007, **72**, 5980; (c) S. M. Park, M. H. Kim, J.-I. Choe, K. T. No and S.-K. Chang, *J. Org. Chem.*, 2007, **72**, 3550; (d) Z. Guo, W. Zhu, L. Shen and H. Tian, *Angew. Chem., Int. Ed.*, 2007, **46**, 5549; (e) S. J. Lee, S. S. Lee, M. S. Lah, J.-M. Hong and J. H. Jung, *Chem. Commun.*, 2006, 4539; (f) S. H. Kim, J. S. Kim, S. M. Park and S.-K. Chang, *Org. Lett.*, 2006, **8**, 371.
- 13 H. S. Jung, P. S. Kwon, J. W. Lee, J. I. Kim, C. S. Hong, J. W. Kim, S. Yan, J. Y. Lee, J. H. Lee, T. Joo and J. S. Kim, *J. Am. Chem. Soc.*, 2009, **131**, 2008.
- 14 International Programme on Chemical Safety, *Hydrogen Sulphide*, World Health Organization, Geneva, Environmental Health Criteria, 19, 1981.
- 15 (a) X. Cao, W. Lin and L. He, *Org. Lett.*, 2011, **13**, 4716; (b) S. A. Patwardhan and S. M. Abhyankar, *Colourage*, 1988, **35**, 15; (c) R. E. Gosselin, R. P. Smith and H. C. Hodge, *Clinical Toxicology of Commercial Products*, Williams and Wilkins, Baltimore, MD, 5th edn, 1984, pp. III-198–III-202.
- 16 R. F. Huang, X. W. Zheng and Y. J. Qu, *Anal. Chim. Acta*, 2007, **582**, 267.
- 17 (a) S. Balasubramanian and V. Pugalenthhi, *Water Res.*, 2000, **34**, 4201; (b) M. F. Choi and P. Hawkins, *Anal. Chim. Acta*, 1997, **344**, 105; (c) F. Maya, J. M. Estela and V. Cerda, *Anal. Chim. Acta*, 2007, **601**, 87; (d) E. A. Guenther, K. S. Johnson and K. H. Coale, *Anal. Chem.*, 2001, **73**, 3481; (e) M. Colon, J. L. Todoli, M. Hidalgo and M. Iglesias, *Anal. Chim. Acta*, 2008, **609**, 160; (f) N. S. Lawrence, R. P. Deo and J. Wang, *Anal. Chim. Acta*, 2004, **517**, 131; (g) C. Giuriati, S. Cavalli, A. Gorni, D. Badoocco and P. Pastore, *J. Chromatogr. A*, 2004, **1023**, 105.
- 18 (a) X. Cao, W. Lin and L. He, *Org. Lett.*, 2011, **13**, 4716; (b) D. Jimenez, R. Martinez-Mañez, F. Sancenon, J. V. Ros-Lis, A. Benito and J. Soto, *J. Am. Chem. Soc.*, 2003, **125**, 9000.
- 19 (a) R. Martinez-Mañez and F. Sancenon, *Chem. Rev.*, 2003, **103**, 4419; (b) E. J. O’Neil and B. D. Smith, *Coord. Chem. Rev.*, 2006, **250**, 3068.
- 20 (a) X. D. Lou, J. G. Qin and Z. Li, *Analyst*, 2009, **134**, 2071; (b) S. Rochat and K. Severin, *Chem. Commun.*, 2011, **47**, 4391; (c) J. S. Wu, R. L. Sheng, W. M. Liu, P. F. Wang, J. J. Ma, H. Y. Zhang and X. Q. Zhuang, *Inorg. Chem.*, 2011, **50**, 6543; (d) L. Zhang, X. Lou, Y. Yu, J. Qin and Z. Li, *Macromolecules*, 2011, **44**, 5186; (e) D. P. Pluth, M. R. Chan, L. E. McQuade and S. J. Lippard, *Inorg. Chem.*, 2011, **50**, 9385; (f) J. Chen, Y. Li, W. Zhong, Q. Hou, H. Wang, X. Sun and P. Yi, *Sens. Actuators, B*, 2015, **206**, 230; (g) Q. Zhou, Y. Zhu, P. Sheng, Z. Wu and Q. Cai, *RSC Adv.*, 2014, **4**, 46951; (h) F. Hou, J. Cheng, P. Xi, F. Chen, L. Huang, G. Xie, Y. Shi, H. Liu, D. Bai and Z. Zeng, *Dalton Trans.*, 2012, **41**, 5799; (i) C. Gao, X. Liu, X. Jin, J. Wu, Y. Xie, W. Liu, X. Yao and Y. Tang, *Sens. Actuators, B*, 2013, **185**, 125; (j) C. Kar, M. D. Adhikari, A. Ramesh and G. Das, *Inorg. Chem.*, 2013, **52**, 743; (k) L. Tang, M. Cai, Z. Huang, K. Zhong, S. Hou, Y. Bian and R. Nandhakumar, *Sens. Actuators, B*, 2013, **185**, 188.
- 21 (a) K. Sasakura, K. Hanaoka, N. Shibuya, Y. Mikami, K. Kimura, T. Komatsu, T. Ueno, T. Terai, H. Kimura and T. Nagano, *J. Am. Chem. Soc.*, 2011, **133**, 18003; (b) F. P. Hou, L. Huang, P. X. Xi, J. Cheng, X. F. Zhao, G. Q. Xie, Y. J. Shi, F. J. Cheng, X. J. Yao, D. C. Bai and Z. Z. Zeng, *Inorg. Chem.*, 2012, **51**, 2454.
- 22 A. K. Mahapatra, S. K. Manna, D. Mandal and C. D. Mukhopadhyay, *Inorg. Chem.*, 2013, **52**, 10825.
- 23 (a) A. K. Mahapatra, S. K. Manna, S. K. Mukhopadhyay and A. Banik, *Sens. Actuators, B*, 2013, **183**, 350; (b) A. K. Mahapatra, J. Roy, P. Sahoo, S. K. Mukhopadhyay and A. Chattopadhyay, *Org. Biomol. Chem.*, 2012, **10**, 2231; (c) A. K. Mahapatra, S. K. Manna, C. D. Mukhopadhyay and D. Mandal, *Sens. Actuators, B*, 2014, **200**, 123; (d) A. K. Mahapatra, S. K. Manna, K. P. Maiti, R. K. Maji, C. D. Mukhopadhyay, D. Sarkar and T. K. Mondal, *RSC Adv.*, 2014, **4**, 36615.
- 24 (a) X. Zhang, Y. Xiao and X. Qian, *Angew. Chem., Int. Ed.*, 2008, **47**, 8025; (b) X. Peng, J. Du, J. Fan, J. Wang, Y. Wu, J. Zhao, S. Sun and T. Xu, *J. Am. Chem. Soc.*, 2007, **129**, 1500; (c) Z. Zhang, D. Wu, X. Guo, X. Qian, Z. Lu, Q. Xu, Y. Yang, L. Duan, Y. He and Z. Feng, *Chem. Res. Toxicol.*, 2005, **18**, 1814; (d) A. Helal, M. H. O. Rashid, C.-H. Choi and H.-S. Kim, *Tetrahedron*, 2012, **68**, 647.
- 25 H. S. Jung, J. H. Han, Y. Habata, C. Kang and J. S. Kim, *Chem. Commun.*, 2011, **47**, 5142.

- 26 Bruker. *APEX2, SAINT and SADABS*. Bruker AXS Inc., Madison, WI, USA, 2009.
- 27 (a) J.-S. Wu, W.-M. Liu, X.-Q. Zhuang, F. Wang, P.-F. Wang, S.-L. Tao, X.-H. Zhang, S.-K. Wu and S.-T. Lee, *Org. Lett.*, 2007, **9**, 33; (b) A. Z. Weller, *Elektrochim.*, 1956, **60**, 1144; (c) A. Weller, *Prog. React. Kinet.*, 1961, **1**, 188.
- 28 (a) J. Cheng, X. Ma, Y. Zhang, J. Liu, X. Zhou and H. Xiang, *Inorg. Chem.*, 2014, **53**, 3210; (b) L. Wang, W. Qin and W. Liu, *Inorg. Chem. Commun.*, 2010, **13**, 1122; (c) J. Wu, W. Liu, J. Ge, H. Zhang and P. Wang, *Chem. Soc. Rev.*, 2011, **40**, 3483.
- 29 (a) Y. Zhou, F. Wang, Y. Kim, S.-J. Kim and J. Yoon, *Org. Lett.*, 2009, **11**, 4442; (b) Z. Xu, Y. Xiao, X. Qian, J. Cui and D. Cui, *Org. Lett.*, 2005, **7**, 889; (c) T. Gunnlaugsson, J. P. Leonard and N. S. Murray, *Org. Lett.*, 2004, **6**, 1557; (d) L. Tang, P. Zhou, K. Zhong and S. Hou, *Sens. Actuators, B*, 2013, **182**, 439.
- 30 K. C. Ko, J.-S. Wu, H. J. Kim, P. S. Kwon, J. W. Kim, R. A. Bartsch, J. Y. Lee and J. S. Kim, *Chem. Commun.*, 2011, **47**, 3165.
- 31 R. K. Pathak, V. K. Hinge, A. Rai, D. Panda and C. P. Rao, *Inorg. Chem.*, 2012, **51**, 4994.
- 32 (a) A. D. Becke, *J. Chem. Phys.*, 1993, **98**, 5648; (b) C. Lee, W. Yang and R. G. Parr, *Phys. Rev. B: Condens. Matter*, 1988, **37**, 785; (c) D. Andrae, U. Haeussermann, M. Dolg, H. Stoll and H. Preuss, *Theor. Chim. Acta*, 1990, **77**, 123.
- 33 P. J. Hay and W. R. Wadt, *J. Chem. Phys.*, 1985, **82**, 299.
- 34 (a) R. K. Harris and P. Jackson, *J. Phys. Chem. Solids*, 1987, **48**, 813; (b) T. H. Lu, P. Chattopadhyay, F. L. Liao and J. M. Lo, *Anal. Sci.*, 2001, **17**, 905; (c) K. R. Anumula, *Anal. Biochem.*, 2006, **350**, 1.
- 35 H. S. Jung, J. H. Han, Z. H. Kim, C. Kang and J. S. Kim, *Org. Lett.*, 2011, **13**, 5056.
- 36 M. J. Frisch, G. W. Trucks, H. B. Schlegel, G. E. Scuseria, M. A. Robb, J. R. Cheeseman, G. Scalmani, V. Barone, B. Mennucci, G. A. Petersson, H. Nakatsuji, M. Caricato, X. Li, H. P. Hratchian, A. F. Izmaylov, J. Bloino, G. Zheng, J. L. Sonnenberg, M. Hada, M. Ehara, K. Toyota, R. Fukuda, J. Hasegawa, M. Ishida, T. Nakajima, Y. Honda, O. Kitao, H. Nakai, T. Vreven, J. A. Montgomery, Jr., J. E. Peralta, F. Ogliaro, M. Bearpark, J. J. Heyd, E. Brothers, K. N. Kudin, V. N. Staroverov, T. Keith, R. Kobayashi, J. Normand, K. Raghavachari, A. Rendell, J. C. Burant, S. S. Iyengar, J. Tomasi, M. Cossi, N. Rega, J. M. Millam, M. Klene, J. E. Knox, J. B. Cross, V. Bakken, C. Adamo, J. Jaramillo, R. Gomperts, R. E. Stratmann, O. Yazayev, A. J. Austin, R. Cammi, C. Pomelli, J. W. Ochterski, R. L. Martin, K. Morokuma, V. G. Zakrzewski, G. A. Voth, P. Salvador, J. J. Dannenberg, S. Dapprich, A. D. Daniels, O. Farkas, J. B. Foresman, J. V. Ortiz, J. Cioslowski and D. J. Fox, *Gaussian 09, Revision D.01*, Gaussian, Inc., Wallingford, CT, 2013.